Wind and Structures, Vol. 10, No. 1 (2007) 45-60
DOI: http://dx.doi.org/10.12989/was.2007.10.1.045

Probability density evolution analysis on dynamic response and reliability estimation of wind-excited transmission towers

Lin-lin Zhang† and Jie Li‡

Department of Building Engineering, School of Civil Engineering, Tongji University, Siping Road 1239, Shanghai, 200092, China

(Received November 15, 2005, Accepted November 3, 2006)

Abstract. Transmission tower is a vital component in electrical system. In order to accurately compute the dynamic response and reliability of transmission tower under the excitation of wind loading, a new method termed as probability density evolution method (PDEM) is introduced in the paper. The PDEM had been proved to be of high accuracy and efficiency in most kinds of stochastic structural analysis. Consequently, it is very hopeful for the above needs to apply the PDEM in dynamic response of wind-excited transmission towers. Meanwhile, this paper explores the wind stochastic field from stochastic Fourier spectrum. Based on this new viewpoint, the basic random parameters of the wind stochastic field, the roughness length z_0 and the mean wind velocity at 10 m heigh U_{10}, as well as their probability density functions, are investigated. A latticed steel transmission tower subject to wind loading is studied in detail. It is shown that not only the statistic quantities of the dynamic response, but also the instantaneous PDF of the response and the time varying reliability can be worked out by the proposed method. The results demonstrate that the PDEM is feasible and efficient in the dynamic response and reliability analysis of wind-excited transmission towers.

Keywords: transmission towers; wind; stochastic Fourier spectrum; probability density evolution; dynamic response; reliability.

1. Introduction

More and more transmission towers, especially large power transmission towers, have recently been built in China based on the increasing power demands. To minimize the risk of disruption to power supply system that may result from in-service tower failure, it is necessary to accurately assess the dynamic response and reliability of the towers subject to wind-loading.

In the past decades, several approaches, including the Monte Carlo method (Shinozuka 1972), the traditional random vibration analysis method (Crandall and Mark 1958) and the virtual excitation method (Lin, *et al*. 1994), have been developed to determine the second-order statistical quantities of structural dynamic response, such as the mean, the standard deviation etc. As far as the

† PhD, E-mail: fatlinwang@163.com
‡ Professor, Corresponding Author, E-mail:lijie@mail.tongji.edu.cn

probability density function of the response is concerned, however, these methods will be limited. In addition, the dynamic reliability of stochastic structures is usually assessed by the level crossing theory through the Rice formula or by the diffusion theory through the backward Kolmogorov equation (Crandall 1970). However, it is found that only approximate dynamic reliability can be obtained by these methods. This is because the joint probability density function of the response and its velocity required in the Rice formula is usually unavailable and can only be assumed, say, to be normal or Rayleigh distribution, with the acquired mean and the standard deviation, and Poisson or Markov assumption in the traditional dynamic reliability analysis may lead to irreducible error. Moreover, although the diffusion process theory based method may give more accurate results, it is still difficult to apply to practical multi-degree of freedom (MDOF) systems. In recent years, a class of probability density evolution method (PDEM), which had been verified to be applicable to stochastic response and dynamic reliability analysis of general MDOF systems, has been developed (Li and Chen 2003, 2005, 2006a, 2006b, Chen and Li 2005). In the method, a genaral probability density evolution equation is deduced for stochastic structural response analysis. This equation holds for any response or index of the structure and the solution will put out the instantaneous probability density function. To evaluate the reliability, an absorbing boundary condition corresponding to the failure criterion is imposed on the probability density evolution equation, solving the equation and integrating over the safe domain will give the dynamic reliability without inducing additional computational efforts compared with the dynamic response analysis.

In the application of the PDEM, the random parameters involved in the wind stochastic field, which reflect the uncertainty in the physical parameters of the structures or the excitations, should be explored and estimated. Clearly, the traditional random process theory, which deals with the random process through their numerical characteristics, can not be used to solve this problem. Therefore, the wind stochastic field is introduced in this paper from the viewpoint of stochastic Fourier spectrum, which has been developed recently by author (Li and Zhang 2004).

The main objective of this paper is to investigate the dynamic response and reliability of wind-excited steel transmission towers by applying the PDEM, together with the stochastic Fourier spectrum model for the wind engineering field. Herein, a wind-excited steel transmission tower, which is supposed to be linear and elastic, is taken as an experimental example. However, in order to make the problem easier, many complex aerodynamic problems, such as wind-structure interaction, buffeting problem and so on, are not considered in the example. In the paper, the mean and the standard deviation of the dynamic response as well as the PDF at certain time instants are evaluated. The reliability and the probability transition of structural responses are also depicted. By the case study, it is founded that the PDEM is feasible and efficient in the dynamic response and reliability analysis of wind-excited transmission towers.

2. Stochastic dynamic response and reliability analysis

2.1. General evolutionary PDF equation of dynamic responses

Until now, there have been several ways for deriving the general probability density evolution equation (Li and Chen 2005, 2006a, b). Herein, one of them, which is the most convenient and directly, is introduced in the following.

Without loss of generality, consider the equation of motion of a MDOF system subject to the wind loading as follows:

$$\mathbf{M}\ddot{\mathbf{X}} + \mathbf{C}\dot{\mathbf{X}} + \mathbf{K}\mathbf{X} = \mathbf{f}(\mathbf{Z}, t) \tag{1}$$

The system has n-degrees-of-freedom, so that the vector $\mathbf{X}$ is a $n \times 1$ displacement response vector, and $\mathbf{M}$, $\mathbf{C}$ and $\mathbf{K}$ are $n \times n$ mass, damping and stiffness matrices, respectively. The overhead dot denotes differentiation with respect to time, t. $\mathbf{f}$ is a $n \times 1$ forcing function vector, and $\mathbf{Z}$ is a $n_Z \times 1$ random parameter vector which reflects the uncertainty in the wind loading, with the known probability density function $p_{\mathbf{Z}}(\mathbf{z})$.

As usual the structure responses with a deterministic initial condition

$$\mathbf{X}(t_0) = \mathbf{x}_0, \quad \dot{\mathbf{X}}(t_0) = \dot{\mathbf{x}}_0 \tag{2}$$

The response $\mathbf{X}(t)$ is obviously a random process dependent on and determined by $\mathbf{Z}$, and can be expressed in a formal expression

$$\mathbf{X}(t) = \mathbf{H}(\mathbf{Z}, t) \tag{3}$$

where $\mathbf{H}$, existent and unique for a well-posed problem, is a deterministic operator. Its component expression is

$$X_j(t) = H_j(\mathbf{Z}, t), \quad j = 1, 2, \cdots, n \tag{4}$$

It should be pointed out that the explicit expression of $\mathbf{H}$ is usually unavailable except for some special simple problem, despite the existence of Eq. (3) and Eq. (4). As far as practical engineering problems are concerned, Eq. (3) and Eq. (4) just provide a deterministic relationship between $\mathbf{Z}$ and $\mathbf{X}$. Taking the above physical solution as Eq. (4), the joint conditional PDF of $X_j(t)$ on the condition $\mathbf{Z} = \mathbf{z}$ is

$$p_{X_j|\mathbf{Z}}(x_j, t|\mathbf{z}) = \delta(x_j - H_j(\mathbf{z}, t)) \tag{5}$$

where $\delta(\ )$ is the Dirac's function.

Thereby, the joint PDF $p_{X_j\mathbf{Z}}(x_j, \mathbf{z}, t)$ is

$$p_{X_j\mathbf{Z}}(x_j, \mathbf{z}, t) = p_{X_j|\mathbf{Z}}(x_j, t|\mathbf{z})p_{\mathbf{z}}(\mathbf{z}) = \delta(x_j - H_j(\mathbf{z}, t))p_{\mathbf{z}}(\mathbf{z}) \tag{6}$$

and the PDF $p_{X_j}(x_j, t)$ is then

$$p_{X_j}(x_j, t) = \int_{\Omega_{\mathbf{z}}} \delta(x_j - H_j(\mathbf{z}, t))p_{\mathbf{z}}(\mathbf{z})d\mathbf{z} \tag{7}$$

Differentiating Eq. (6) with respect to t on both sides will lead to

$$\begin{aligned} \frac{\partial p_{X_j\mathbf{Z}}(x_j, \mathbf{z}, t)}{\partial t} &= \frac{\partial[\delta(x_j - H_j(\mathbf{z}, t))p_{\mathbf{z}}(\mathbf{z})]}{\partial t} \\ &= p_{\mathbf{Z}}(\mathbf{z})\frac{\partial[\delta(x_j - H_j(\mathbf{z}, t))]}{\partial t} \end{aligned}$$

$$= -p_{\mathbf{Z}}(\mathbf{z})\dot{H}_j(\mathbf{z}, t)\frac{\partial[\delta(x_j - H_j(\mathbf{z}, t))]}{\partial x}$$

$$= -\dot{H}_j(\mathbf{z}, t)\frac{\partial[\delta(x_j - H_j(\mathbf{z}, t))p_{\mathbf{z}}(\mathbf{z})]}{\partial x}$$

$$= -\dot{H}_j(\mathbf{z}, t)\frac{\partial p_{X_j\mathbf{Z}}(x_j, \mathbf{z}, t)}{\partial x} \tag{8}$$

Then, the probability density evolution equation will be derived as following

$$\frac{\partial p_{X_j\mathbf{Z}}(x_j, \mathbf{z}, t)}{\partial t} + \dot{H}_j(\mathbf{z}, t)\frac{\partial p_{X_j\mathbf{Z}}(x_j, \mathbf{z}, t)}{\partial x} = 0 \tag{9}$$

where $\dot{H}_j(\mathbf{z}, t) = \dot{X}_j(t)$ is the 'velocity' of the response for a prescribed **z**. Analogous to the **H**, the explicit expression of $\dot{H}_j(\mathbf{z}, t)$ is also unavailable. But then it will be found in the numerical algorithm that only the value of the $\dot{H}_j(\mathbf{z}, t)$ is used. In other words, as long as it is numerically tractable, the PDF $p_{X_j\mathbf{Z}}(x_j, \mathbf{z}, t)$ is numerically solvable from Eq. (9) with the initial condition

$$p_{X_j\mathbf{Z}}(x_j, \mathbf{z}, t) = \delta(x_j - x_{j,0})p_{\mathbf{z}}(\mathbf{z}), \text{ for } t = t_0 \tag{10}$$

where $x_{j,0}$ is the deterministic initial value of $X_j(t)$.

Finally, the PDF of $X_j(t)$ reads

$$p_{X_j}(x_j, t) = \int_{\Omega_{\mathbf{z}}} p_{X_j\mathbf{Z}}(x, \mathbf{z}, t)d\mathbf{z} \tag{11}$$

in which $\Omega_{\mathbf{Z}}$ is the distribution domain of **Z**.

2.2. Dynamic reliability assessment

Essentially, Eq. (9) is a conservative equation, which implies the principle of preservation of probability is valid for a single random event (Li and Chen 2006). This significance of this physical sense will be seen in the part.

In traditional dynamic reliability theory, limited by the available stochastic response analysis methods, a level-crossing process with Poisson assumption or Markov assumption is constructed for the first passage problem. On the other hand, the PDEM provides another way to the dynamic reliability analysis.

As well known, the dynamic reliability about the dynamic response $X_j(t)$ can be expressed as

$$R(t) = P\{X_j(\tau) \in \Omega_S, \quad \tau \in [0, t]\} \tag{12}$$

where $P\{\cdot\}$ is the probability of the random event; Ω_S is the safe domain.

Eq. (12) suggests that the dynamic reliability is the total probability of the dynamic response $X_j(t)$ that is always in the safe domain over the time interval $[0, t]$. Otherwise, once the random events enter the failure domain, the related probability will never return to the safe domain. That is, the probability density transits one-direction outside the boundary. As a result, an absorbing boundary condition may be introduced in Eq. (9), i.e.,

$$p_{X_j\mathbf{Z}}(x_j, \mathbf{z}, t) = 0, \qquad x_j \in \Omega_\mathrm{f} \tag{13}$$

where Ω_f is the failure domain.

Therefore, the dynamic reliability problem can be solved as an initial-boundary-value partial differential equation problem. Denoting the solution of the initial-boundary-value problem (9), (10) and (13) as $\breve{p}_{X\mathbf{Z}}(x, \mathbf{z}, t)$, the "remaining" PDF is (Chen and Li 2005)

$$\breve{p}_{X_j}(x_j, t) = \int_{\Omega_\mathbf{z}} \breve{p}_{X_j\mathbf{Z}}(x, \mathbf{z}, t)d\mathbf{z} \tag{14}$$

and the reliability will be given by

$$R(t) = \int_{\Omega_\mathrm{S}} \breve{p}_{X_j}(x_j, t)dx_j \tag{15}$$

For the symmetrical double boundary problem, Eq. (13) becomes

$$R(t) = \int_{-x_{\mathrm{j,B}}}^{x_{\mathrm{j,B}}} \breve{p}_{X_j}(x_j, t)dx_j \tag{16}$$

It is obvious that it becomes the dynamic response analysis problem when $x_{\mathrm{j,B}} \to \infty$.

2.3. Numerical solving algorithm

As mentioned above, it's very difficult to compute the analytical solution of dynamic response and reliability. The numerical solving algorithm is recommended by Li and Chen (2005) is used herein. Its basic solving procedure is shown as follows:

Step 1. Discretize $\mathbf{z}$ in the domain $\Omega_\mathbf{Z}$ and denote the lattice point as $\mathbf{z}_q$, $q=1,2,\ldots,N_s$, where N_s is the total number of the discretized representative points.

Step 2. For a given $\mathbf{z}_q$, solve Eq. (1) with a deterministic time integration method to obtain the velocity $\dot{X}(\mathbf{z}_q, t_m)$, in which $t_m = m \cdot \Delta t$ and Δt is the time step.

Step 3. Solve the initial-boundary-value problem defined by Eqs. (9), (10) and (13) with the finite difference method.

Step 4. Carry out the numerical integration in Eq. (11) for the dynamic response analysis, or in Eq. (15) for reliability assessment.

It is mentioned in the solving steps 1-4 that a routine deterministic analysis is applied in Step 2 to compute the coefficient of the probability density evolution equation, and a finite difference method is used in Step 3 to obtain the PDF. In this paper, Newmark Beta time integration method (Clough and Penzien 1993) is adopted for the deterministic dynamic response analysis.

With the TVD scheme (Shen, Zhang and Niu 2001), Eq. (9) is changed into the following discretized form

$$\begin{aligned} p_{j,k+1} &= p_{j,k} - r_L\left[\frac{1}{2}(g_k + |g_k|)(p_{j,k} - p_{j-1,k}) + \frac{1}{2}(g_k - |g_k|)(p_{j+1,k} - p_{j,k})\right] \\ &-\frac{1}{2}(1 - |r_L g_k|)|r_L g_k|[\psi(r^+_{j+1/2}, r^-_{j+1/2})(p_{j+1,k} - p_{j,k}) \\ &-\psi(r^+_{j-1/2}, r^-_{j-1/2})(p_{j,k} - p_{j-1,k})] \end{aligned} \tag{17}$$

where $p_{j,k}$ denotes $p_{X_j\mathbf{Z}}(x_j, \mathbf{z}_q, t_k)$ for simplicity; $t_k = k \cdot \Delta\hat{t}$ and $\Delta\hat{t}$ is the time step in the difference method; $r_L = \Delta\hat{t}/\Delta x$ is the lattice ratio; $r^+_{j+1/2} = (p_{j+2,k} - p_{j+1,k})/(p_{j+1,k} - p_{j,k})$, $r^-_{j+1/2} = (p_{j,k} - p_{j-1,k})/(p_{j+1,k} - p_{j,k})$, $r^+_{j-1/2} = (p_{j+1,k} - p_{j,k})/(p_{j,k} - p_{j-1,k})$, $r^-_{j-1/2} = (p_{j-1,k} - p_{j-2,k})/(p_{j,k} - p_{j-1,k})$ is the flux limiter, and

$$g_k = \frac{1}{2}[\dot{X}_k(\mathbf{z}_q, t_{k-1}) + \dot{X}_j(\mathbf{z}_q, t_k)] \tag{18}$$

The Courant-Friedrichs-Lewy condition (CFL) for Eq. (17) reads

$$|r_L g_k| \le 1 \tag{19}$$

The Roe-Sweby flux limiter with relatively small dissipation is adopted to construct the flux limiter in Eq. (17).

$$\psi_{sb}(r^-) = \max(0, \min(2r^-, 1), \min(r^-, 2)) \tag{20}$$

As the time dependent property of $\dot{X}_j(\mathbf{z}, t)$, the following form of the employed flux limiter, which should have an adaptive ability to choose the difference direction, is used

$$\psi(r^+, r^-) = u(-g_k)\,\psi_{sb}(r^+) + u(g_k)\,\psi_{sb}(r^-) \tag{21}$$

where $u(\ )$ is the Heaviside function

$$u(x) = \begin{cases} 1, & \text{for } x \ge 0 \\ 0, & \text{otherwise} \end{cases} \tag{22}$$

Within the finite difference solution, the initial condition Eq. (10) should also be discretized in the finite difference solution. Its discretized form is

$$p_{X_j\mathbf{Z}}(x_j, \mathbf{z}_q, t_0) = \begin{cases} \frac{1}{\Delta x}\bar{p}_{\mathbf{Z}}(\mathbf{z}_q), & \text{for } x_j \in \left[x_0 - \frac{1}{2}\Delta x, x_0 + \frac{1}{2}\Delta x\right] \\ 0, & \text{otherwise} \end{cases} \tag{23}$$

where $x_j = j \cdot \Delta x$, $j = 0, \pm 1, \pm 2, \cdots$, Δx is the space step in x direction. $\bar{p}_{\mathbf{Z}}(\mathbf{z}_q)$ is the nominal PDF related to $p_{\mathbf{Z}}(\mathbf{z})$. Only if the uniformly meshing strategy of selecting points were used, $\bar{p}_{\mathbf{Z}}(\mathbf{z}_q) = p_{\mathbf{Z}}(\mathbf{z}_q)$. Otherwise, $\bar{p}_{\mathbf{Z}}(\mathbf{z}_q)$ is determined by the strategy of selecting points and $p_{\mathbf{Z}}(\mathbf{z})$.

3. Stochastic wind spectrum model

The PDEM introduced as above only give a possible way to catch the instantaneous PDF of the response and the reliability of given structures. However, it has not given the input model for wind-excited structures. To settle this requirement, Li and Zhang investigated and proposed a new model named as Stochastic Fourier Spectrum of wind velocity fluctuation (Li and Zhang 2004). It is described briefly in the following section.

3.1. Power spectrum density model

Typically, a mean velocity $\bar{\mathbf{v}}$ and three fluctuating components $\mathbf{v}(t)$ of velocity in three mutually perpendicular directions can characterize the wind flow at a given point in space. To a given period, the mean velocity can be regarded as steady. By contraries, one of the most recognizable features of the fluctuating velocity is that it is a stochastic process. From the traditionally point of view, the power spectra and cross-spectra of velocity of the process, which are alternative to and interchangeable with the correlation functions, seem important.

Since 1960s, a number of empirical spectrum models of the longitudinal gustiness in winds have been presented, such as Von Karman spectrum, Davenport spectrum, Simiu spectrum, etc (Simiu and Scanlan 1978). Most of them are based on the Kolmogorov theory, which defines a general PSD form of the fluctuating wind velocity shown as follows.

$$\frac{nS(z,n)}{u_*^2} = \frac{Af^{\gamma}}{(1+Bf^{\alpha})^{\beta}} \tag{24}$$

where n is frequency, u_* is shear velocity and f is the so-called Mooning coordinates. A, B, α, β and γ are coefficients dependant on the measured data and assumptions used in different models.

For practical applications, different measured data would introduce different empirical spectra. For example, Davenport chose about 70 spectra of the horizontal components of gustiness in strong winds and other published data, and presented the famous Davenport spectrum for strong winds in the lower layers (Davenport 1961). Its expression is

$$\frac{nS(z,n)}{u_*^2} = \frac{4f^2}{(1+f^2)^{4/3}} \tag{25}$$

where $f = 1200\omega/(2\pi U_{10})$, U_{10} is the mean wind velocity at 10 m height.

Originally, the expression of Eq. (25) was proposed by trial, through which it was found that this expression was fit satisfactorily to the points according to the above mentioned data (see Fig. 1). From Fig. 1, it can be recognized that Davenport spectrum just is a mean reflection to the physical relationship between the PSD function S and the frequency n. However, the empirical models can not disclose the physical essence of the randomness in the wind process. To tackle this problem, an idea of stochastic Fourier spectrum, which tries to reflect the random process based on the physical relationship between observed phenomena, was proposed in the following.

3.2. Stochastic fourier spectrum

As well known, there are two methods used to describe a given time series. One is the time

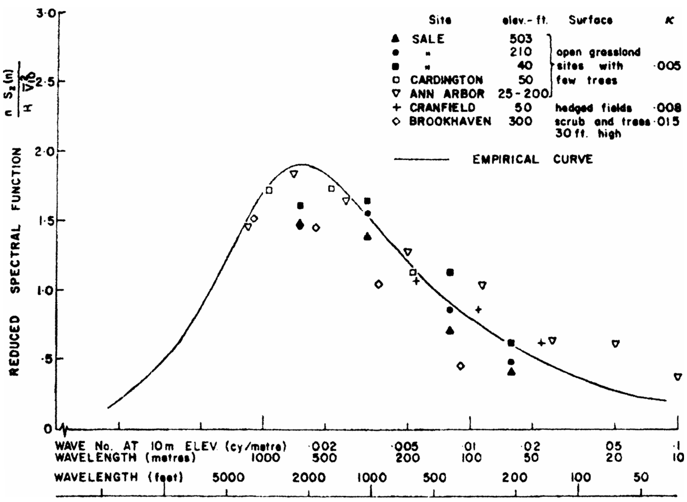

Fig. 1 Davenport empirical spectrum of horizontal gustiness in high winds

process, and the other is the spectrum in frequency domain. They connect with each other through Fourier transform. In other words, the sample functions of the Fourier spectrum $F(\omega)$ can be computed from those of the wind fluctuation time process by the Fourier transform, and on the contrary. Therefore, the random Fourier Spectrum can be defined as a set of sample functions of the Fourier spectrum obtained in a set of experiments.

Usually, the Fourier spectrum $F(\omega)$ is separated into two kinds of spectrum functions, that is, Fourier amplitude spectrum and Fourier phase spectrum. Taking Fourier amplitude spectrum as a random function, in which the basic random variables is some measurable physical parameters such as the roughness length z_0 and the mean wind velocity at 10 m height U_{10}, will give the stochastic Fourier spectrum (Li and Zhang 2004). For a stationary process, the power spectrum of a stochastic Fourier spectrum can be computed by the following expression

$$S(\omega) = \frac{1}{T} E[|F(\omega)|^2] \tag{26}$$

where $|F(\omega)|$ is the Fourier amplitude spectrum, T is the duration of the sample functions, and ω is the angular frequency.

Therefore, the formal expression of the stochastic Fourier spectrum could be expressed as

$$F(\omega, \lambda, \xi, \ldots) = \sqrt{S(\omega, \lambda, \xi, \ldots)} \tag{27}$$

where $\lambda, \xi, \ldots$ are basic measurable physical parameters, which are treated as random variables in the stochastic Fourier amplitude spectrum according to its practical physical background. By means of statistics, the PDFs of these random variables can be obtained.

In this paper, the stochastic Fourier spectrum is adopted as (Li and Zhang 2004)

$$F(\omega) = \sqrt{\frac{11672.2\,\omega}{[\ln(10/z_0)]^2 \times \left[1 + \left(\frac{1200\,\omega}{2\pi U_{10}}\right)^2\right]^{\frac{4}{3}}}} \tag{28}$$

where z_0 is the roughness length and U_{10} is the mean wind velocity at 10 m height.

3.3. The PDFs of the random variables

According to the definition in Eq. (28), the roughness length z_0 and the mean wind velocity at 10 m height U_{10} should be regarded as the random variables. As well known, in the planetary boundary layer, the wind at a point is characterized first by the large-scale movements of the pressure systems giving rise to the gradient wind and then by the modifying influence of the ground surface. Generally, the second process can be characterized by the roughness length z_0. And the mean wind velocity at 10 m height U_{10} can also be related with the gradient wind by the wind velocity profile, such as logarithmic profile and power law profile. Hence, these two parameters are able to be taken to explain the randomness of the wind field in the boundary layer. In other words, their randomness properties give rise to variations in wind velocity.

The PDFs of z_0 and U_{10} can be investigated by means of statistics. The results are (Li and Zhang 2004)

$$f_{z_0}(z_0) = \begin{cases} \dfrac{0.262}{z_0}\exp(-0.216(\ln z_0 + 3.507)^2) & z_0 \geq 0 \\ 0 & z_0 < 0 \end{cases} \tag{29}$$

$$f_{U_{10}}(U_{10}) = 0.265 * \exp\{-\exp[-0.265(U_{10} - 24.872)]\} * \exp[-0.265(U_{10} - 24.872)] \tag{30}$$

where the mean and rms values of the roughness length z_0 are 0.09 m and 0.20 m, and those of the mean wind speed at 10 m height U_{10} are 27.05 m/s and 4.84 m/s.

4. Model of multivariate wind stochastic field

As is stated earlier, the wind velocity of a given point consists of two parts, encompassing the mean wind velocity $\bar{v}_i(z)$ and the fluctuating wind velocity $v_i(z, t)$. It is proved that the fluctuating part $v_i(z_i, t)$ can be simulated by the stochastic Fourier spectrum. For a multivariate wind stochastic field, the stochastic Fourier cross-spectrum matrix $\mathbf{F}(z_0, U_{10}, \omega)$ can be introduced as follows (Zhang and Li 2006).

$$\mathbf{F}(z_0, U_{10}, \omega) = \begin{bmatrix} F_{11}(z_0, U_{10}, \omega) & F_{12}(z_0, U_{10}, \omega) & \cdots & F_{1n}(z_0, U_{10}, \omega) \\ F_{21}(z_0, U_{10}, \omega) & F_{22}(z_0, U_{10}, \omega) & \cdots & F_{2n}(z_0, U_{10}, \omega) \\ \vdots & \vdots & \ddots & \\ F_{n1}(z_0, U_{10}, \omega) & F_{n2}(z_0, U_{10}, \omega) & \cdots & F_{nn}(z_0, U_{10}, \omega) \end{bmatrix} \tag{31}$$

where the diagonal components and the off diagonal components are denoted by the stochastic Fourier amplitude spectrum at the given point j and the coherence function between point i and j as follows:

$$F_{ii}(z_0, U_{10}, \omega) = F_{V_i}(z_0, U_{10}, \omega)^2, \qquad i = 1, 2, \ldots, n \tag{32}$$

$$F_{ij}(z_0, U_{10}, \omega) = F_{V_i}(z_0, U_{10}, \omega)F_{V_j}(z_0, U_{10}, \omega)\gamma_{ij}(\omega), \quad i,j = 1, 2, ..., n, \quad i \neq j \tag{33}$$

in which $\gamma_{ij}(\omega)$ is the coherence function. In this paper, the coherence function presented by Davenport (1968) is used

$$\gamma_{ij}(\omega) = \exp\left(-\frac{|\omega|[C_z^2(z_i - z_j)^2 + C_y^2(y_i - y_j)^2]^{0.5}}{\pi \cdot [\bar{V}(z_i) + \bar{V}(z_j)]}\right) \tag{34}$$

in which $C_z = 10$ and $C_y = 16$.

$$\omega_{ml} = (l-1)\Delta\omega + \frac{m}{n}\Delta\omega, \quad l = 1, 2, ..., N \tag{35}$$

$$\Delta\omega = \omega_u / N \tag{36}$$

In Eq. (36), ω_u is an upper cutoff frequency beyond which the element of the stochastic Fourier cross-spectrum matrix may be assumed to be zero for either mathematical or physical reasons. As such, ω_u is a fixed value and hence $\Delta\omega \to 0$ as $N \to \infty$ so that $N\Delta\omega = \omega_u$.

As the fluctuating wind velocity is usually regarded as Gaussian process, the basic ideas of the spectral representation method (Shinozuka and Deodatis 1991, Deodatis 1996) may be introduced to synthesize the fluctuating wind velocity at point j, that is:

$$V_j(t) = \frac{1}{4}\sum_{m=1}^{j}\sum_{l=1}^{N} I_{jm}(\omega_{ml})\sqrt{\Delta\omega}\cos[\omega_{ml}t + \Phi_{ml}], \qquad j = 1, 2, ..., n \tag{37}$$

in which n is the total number of simulating points in the space, and $I_{jm}(\omega_{ml})$ is the non-zero component of a lower triangular matrix $\mathbf{I}(\omega)$, which is obtained by decomposing the stochastic Fourier cross-spectrum matrix $\mathbf{F}(z_0, U_{10}, \omega)$ using Cholesky's method.

The Φ_{ml} appearing in Eq. (37) are independent random phase angles distributed uniformly over the interval $[0, 2\pi]$.

5. The stochastic response and reliability of wind-excited transmission towers

5.1. Basic considerations

According to above background, the stochastic dynamic response of wind-excited transmission towers can be analyzed easier by means of finite element method. A latticed steel transmission tower, which is supposed to be excited by horizontal wind loads and supposed to be linear and elastic in vibration process, is investigated in detail. In order to make the problem easier, the complex aerodynamic behavior, such as wind-structure interaction, buffeting problem and so on, aren't considered in the case. In the modeling process, the three-dimensional structure is simplified to a 2D lumped-mass model. Fig. 2 shows both the 3D model and 2D model. The masses and heights of the sixteen lumped-mass points are shown in the Fig. 2 too. Each two adjacent lumped mass points are jointed by a beam element, whose material and geometric parameters are shown in

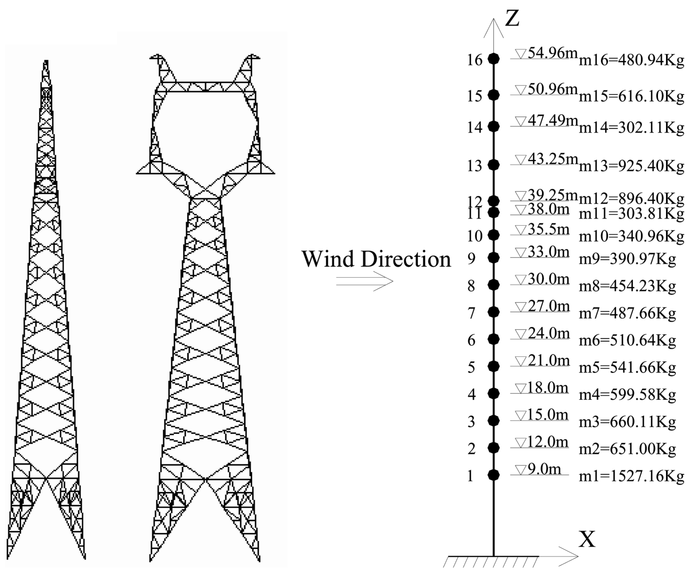

Fig. 2 3D finite element model and 2D lumped-mass model the transmission tower

Table 1 Material parameters of the 2D lumped-mass model

Elastic Modulus (MPa)	Poisson Ratio
210000	0.3

Table 2 Geometry parameters of the 2D lumped-mass model

No. of column	Cross-sectional area (m^2)	Moment of cross-sectional area	
		I_{xx} (m^4)	I_{yy} (m^4)
1	0.8836	0.065062	0.0046295
2	0.8836	0.065062	0.14209
3	0.8836	0.065062	0.12718
4	0.8836	0.065062	0.090846
5	0.8836	0.065062	0.045616
6	0.8836	0.065062	0.0027532
7	0.8836	0.065062	0.00065062
8	0.8836	0.065062	0.00091667
9	0.8836	0.065062	0.0013784
10	0.8836	0.065062	0.00099922
11	0.8836	0.065062	0.00065062
12	0.8836	0.065062	0.032751
13	0.8836	0.065062	0.00065062
14	0.8836	0.065062	0.032892
15	0.8836	0.065062	0.058459
16	0.8836	0.065062	0.064310

Table 1 and Table 2. To save the compute cost, the finite element updating method based on Bayesian estimation and minimization of dynamic residuals (Alvin 1997) is introduced.

The ith component of $\mathbf{f}(t)$ in Eq. (1), neglecting the wind-structure interaction, is given by the following relationship:

$$f_i(t) = \gamma_i(\bar{v}_i + v_i(t))^2 \tag{38}$$

where $\bar{v}_i$ is the mean wind velocity at the point z_i, v_i is the corresponding fluctuating part, and γ_i is a coefficient equal to $0.5\rho\mu_s A_i$, where ρ being the air density, A_i the impact area of the ith node in the direction of the mean wind, μ_s a structural shape factor. In the following example, $\rho = 1.226\ kg/m^3$ and $\mu_s = 0.8$ are adopted.

In the dynamic analysis, as mentioned previously, the roughness length z_0 and the mean wind velocity at 10 m height U_{10} are taken as the random parameters with the PDFs listed as Eq. (29) and Eq. (30). By pre-analysis, it is found that the first-order and second-order natural periods are 0.596 sec and 0.240 sec, respectively. Therefore, if the damping ratio is supposed to be 0.02., then the Rayleigh damping, i.e., $\mathbf{C} = a\mathbf{M} + b\mathbf{K}$, is applied where $a = 0.30088$, $b = 0.00109$. The wind stochastic field is simulated by superposition method introduced upwards.

5.2. Stochastic dynamic response

The mean and the standard deviation of the displacement of the top node in the 2-D model of transmission tower are evaluated by the proposed method. Only 359s is required on the computer with RAM of 256 Mb and CPU of 2.4 GHz. Fig. 3 shows parts of the results. It is shown that the maximum coefficient of variation (COV) of responses reaches 0.446.

Fig. 4 shows the PDF at certain time instants, say, 20.0s, 40.0 and 60.0s. From Fig. 4, the PDFs seem similar to extreme value-I distribution, although the simulated wind field is characteristic of Gaussian. Moreover, the shape of PDF is varying with time. To show this change more clearly, the

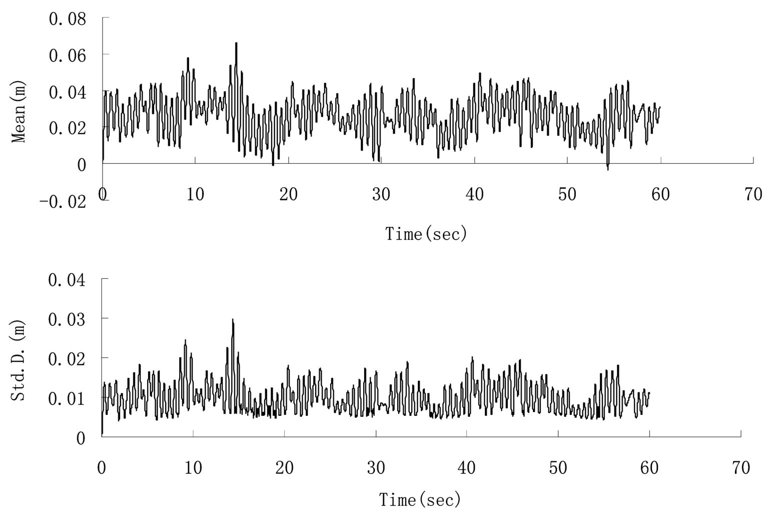

Fig. 3 The comparison of the mean and the standard deviation

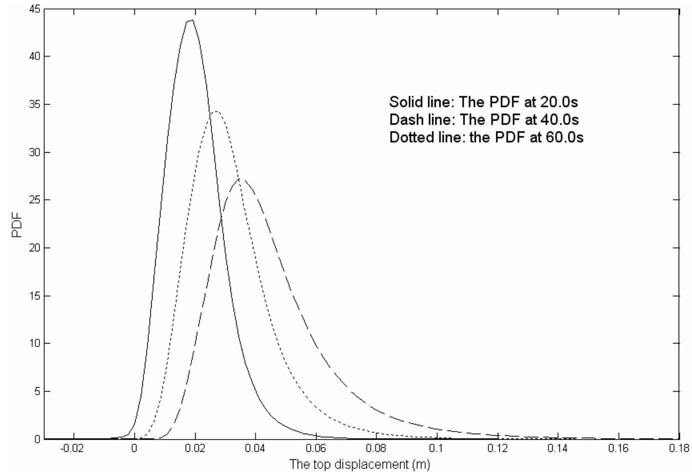

Fig. 4 Typical probability density curves

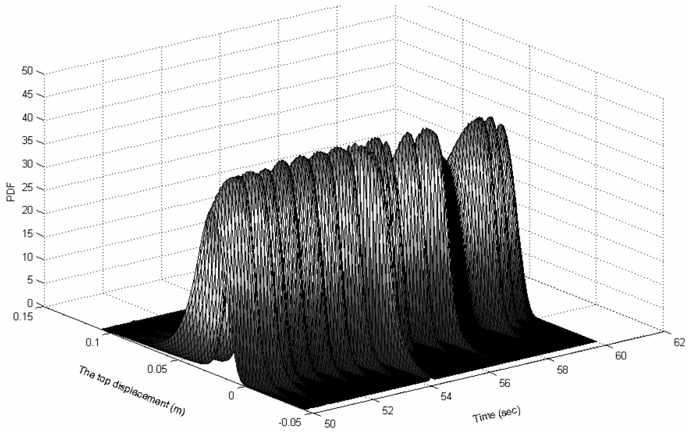

Fig. 5 The PDF surface varying with time

time varying process of the PDF is pictured in Fig. 5. It is seen that the PDFs vary with time irregularly and acutely. Additionally, Fig. 6 shows the contour of the PDF, which seems like a river with some whirlpools.

5.3. Dynamic reliability assessment

The symmetrical double boundary is adopted in the evaluation of the dynamic reliabilities herein. Defining the reliability by the displacement of the top node in the 2-D models, Eq. (12) is substituted by

$$R(t) = P\{|X_{top}(\tau)| \le x_B,\ \tau \in [0, t]\} \tag{39}$$

where $X_{top}(t)$ is the displacement of the top floor.

The reliability in the time interval [0, 60] sec for different boundary is listed in Table 3. As far as

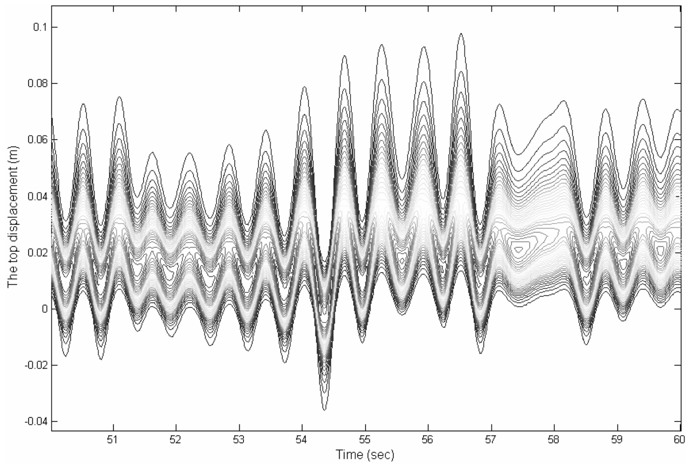

Fig. 6 The PDF counter varying with time

Table 3 The reliabilities under different thresholds

Threshold	Reliability
0.20	0.6122
0.25	0.7215
0.30	0.8017
0.40	0.8965

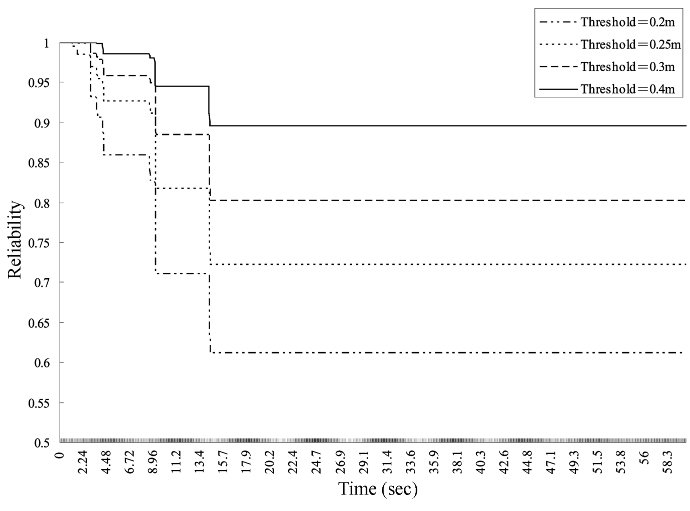

Fig. 7 The time dependent reliabilities

the computational efforts are concerned, the PDEM is as time-saving as the situation in dynamic response analysis, say, only 8174 sec is consumed on the same computer. From the table it is noticed that the reliability decline with the threshold decreasing. In the meantime, from Fig. 7, which depicts the reliabilities varying with time, it is seen that the reliabilities decline with time increasing.

Additionally, the figures in Fig. 7 show that the reliabilities decline not smoothly but usually in a ladder-shape. This might mean that the level-crossing process of the stochastic response under random wind loading is not Poisson or Markovian, the events of level crossing occur in cluster. The reason requires in-depth research.

6. Conclusions

The probability density evolution method is adopted for stochastic dynamic response analysis and reliability estimation of wind-excited transmission towers. The wind stochastic field is studied from the viewpoint of the stochastic Fourier spectrum. A simulation method of the fluctuating wind velocity based on the stochastic Fourier spectrum is introduced. A latticed steel transmission tower subject to the horizontal wind loads is investigated in detail without considering the effects of the wind-structure interaction. Some features of the responses and the reliabilities of the structure are observed and discussed. It is found that the PDEM can be successfully applied in the dynamic response analysis and reliability estimation of wind-excited transmission towers with high efficiency.

Acknowledgements

The support of the Natural Science Funds for Innovative Research Groups of China(Grant No. 50321803) is gratefully acknowledged.

Reference

Alvin, K. F. (1997), "Finite element model update via Bayesian estimation and minimization of dynamic residuals", *AIAA J.*, **35**(5), 879-886.

Chen, J. B. and Li, J. (2005), "Dynamic response and reliability analysis of non-linear stochastic structures", *Probab. Eng. Mech.*, **20**, 33-44.

Clough, R. W. and Penzien, J. (1993), *Dynamics of Structures; 2nd edn*, McGraw-Hill, New York.

Crandall, S. H. and Mark, M. D. (1958), *Random Vibration in Mechanical System,* Academic Press, New York.

Crandall, S. H. (1970), "First-crossing probabilities of the linear oscillator", *J. Sound Vib.*, **12**, 285-299.

Davenport, A. G. (1961), "The spectrum of horizontal gustiness near the ground in high winds", *Q. J. Roy. Meteor. Soc.*, **87**, 194-211.

Davenport, A. G. (1961), "The dependence of wind load upon meteorological parameters", *Proceeding of the International Research Seminar on Wind Effects on Buildings and Structures,* University of Toronto Press, Toronto.

Deodatis, G. (1996), "Simulation of ergodic multivariate stochastic process", *J. Eng. Mech. ASCE*, **122**(8), 91-109.

Li, J. and Chen, J. B. (2003), "Probability density evolution method for dynamic response analysis of stochastic structures", *Proceeding of the Fifth International Conference on Stochastic Structural Dynamics*, Hangzhou, China, August.

Li, J. and Chen, J. B. (2005), "Dynamic response and reliability analysis of structures with uncertain parameters", *Int. J. Num. Meth. Eng.*, **62**, 289-315.

Li, J. and Chen, J. B. (2006a), "The probability density evolution method for dynamic response analysis of non-linear stochastic structures", *Int. J. Num. Meth. Eng.*, **65**, 882-903.

Li, J. and Chen, J. B. (2006b), "The principle of preservation of probability and the generalized density evolution equation", *Structural Safety,* (available on line).

Li, J. and Zhang, L. L. (2004), "A study on the relationship between turbulence power spectrum and stochastic Fourier amplitude spectrum", *J. Disaster Prevention and Mitigation Eng.*, **24**(4), 363-369 [in Chinese].

Lin, J. H., Zhang, W. S., and Li, J. J. (1994), "Structural response to arbitrarily coherent stationary random excitations", *Comput. Struct.*, **50**(5), 629-634

Shinozuka, M. (1972), "Monte-Carlo solution of structural dynamics", *Comput. Struct.*, **2**, 855-874.

Shen, M. Y., Zhang, Z. B., and Niu, X. L. (2001), "Some advances in study of high order accuracy and high resolution finite difference schemes", In *New Advances in Computational Fluid Dynamics*, Dubois, F., Wu, H. M. (eds). Higher Education Press: Beijing.

Shinozuka, M. and Deodatis, G. (1991), "Simulation of stochastic processes by spectral representation", *Appl. Mech. Rev.*, **44**(4), 191-204.

Simiu, E. and Scanlan, R. H. (1978), *Wind Effects on Structures: An Introduction to Wind Engineering,* Wiley, New York.

Tennekes, H. (1973), "The logarithmic wind profile", *J. Atmospheric Sci.*, **30**, 234-238.

Zhang, L. L. and Li, J. (2006), "Research on the cross stochastic Fourier spectrum of turbulence", *J. Architecture and Civil Eng.*, **23**(2), 57-61.

CC